E9-2005-168

E. A. Matyushevsky, N. A. Morozov, E. M. Syresin

CALCULATIONS OF MAGNETIC FIELD ERRORS CAUSED BY MECHANICAL ACCURACY AT INFRA-RED UNDULATOR CONSTRUCTION

Матюшевский Е. А., Морозов Н. А., Сыресин Е. М. E9-2005-168
Расчеты ошибок магнитного поля, вызванных механической точностью конструкции инфракрасного ондулятора

В Объединенном институте ядерных исследований (Дубна) проводится разработка электромагнитного ондулятора с максимальным магнитным полем 1,2 Тл и периодом 40 см. Разработаны компьютерные модели магнитной системы ондулятора на основе программ POISSON и RADIA. При помощи моделей рассчитаны возмущения магнитного поля ондулятора из-за ошибок его изготовления.

Работа выполнена в Лаборатории ядерных проблем им. В. П. Джелепова и Лаборатории высоких энергий им. В. И. Векслера и А. М. Балдина ОИЯИ.

Сообщение Объединенного института ядерных исследований. Дубна, 2005

Matyushevsky E. A., Morozov N. A., Syresin E. M. E9-2005-168
Calculations of Magnetic Field Errors Caused by Mechanical Accuracy at Infra-Red Undulator Construction

At the Joint Institute for Nuclear Research (Dubna) the electromagnetic undulator with maximal magnetic field 1.2 T and 40 cm period is under development. The computer models for the undulator magnet system were realized on the basis of POISSON and RADIA codes. The undulator magnetic field imperfections due to the design errors were simulated by the models.

The investigation has been performed at the Dzhelepov Laboratory of Nuclear Problems and the Veksler and Baldin Laboratory of High Energies, JINR.

Communication of the Joint Institute for Nuclear Research. Dubna, 2005

1. UNDULATOR PARAMETERS

Requirements to undulator magnetic system imperfection caused by a mechanical accuracy at its construction essentially depend on undulator parameters. The undulator parameter K corresponds to

$$K = 93.4 B_{z[T]} \cdot \lambda_{u[m]}.$$

It is equal to $K = 44.8$ at a magnetic field of $B_z = 1.2$ T and an undulator period of $\lambda_u = 40$ cm. The undulator parameter corresponds to $K = 3.7$ at a magnetic field of B_z =1 kG. The wavelength of undulator radiation for the first harmonic is equal to

$$\lambda = \frac{\lambda_u}{2\gamma^2}\left(1 + \frac{K^2}{2}\right).$$

The wavelength corresponds to $\lambda = 100$ μm at an electron energy of 700 MeV and to $\lambda = 1.5$ μm at an electron energy of 500 MeV, a magnetic field of 1 kG.

The diffraction angle and diffraction spot radius of undulator radiation are defined by

$$\theta_d \approx \sqrt{\lambda/\pi L},$$

$$r_d \approx \sqrt{\lambda L/\pi},$$

where $L = 4$ m is the undulator length. The diffraction parameters are equal to $\theta_d \approx 3$ mrad and $r_d \approx$1 cm at a wavelength of $\lambda = 100$ μm. The diffraction angle $\theta_d \approx 3$ mrad is a few times larger than electron transverse kick produced at imperfection of the undulator magnetic system. The imperfection of the magnetic undulator system is characterized by the first and second integrals of vertical dipole field

$$x' = \frac{e}{\gamma mc}\int B_z ds,$$

$$x = \frac{e}{\gamma mc}\int ds \int B_z ds'.$$

According to DESY infra-red undulator specifications, the first integral corresponds to $I_1 = \int B_z ds = 2 \cdot 10^{-4}$ T·m and the second one is $I_2 = \int ds \int B_z ds' =$ $= 2 \cdot 10^{-4}$ T·m^2 at a magnetic field of 0.3–1.2 T. The magnetic system imperfection leads to electron angle divergence of $x' \approx 0.1$ mrad and electron trajectory displacement of $x \approx 0.1$ mm at an electron energy of 0.7 GeV. Both these values are larger by more than one order of magnitude than corresponding diffraction angle θ_d and spot radius r_d.

At the realization of replica application the undulator radiation wavelength is 420 nm – 1 μm at a magnetic field of 1 kG. In this case the diffraction angle and diffraction spot radius are equal to $\theta_d \approx 0.3$ mrad and $r_d \approx 1$ mm at an undulator radiation wavelength of 1 μm. It is one order of magnitude less than the value corresponding to infra-red regime. According to undulator specification, the first and second integrals in this case are equal to $I_1 = \int B_z ds = 10^{-4}$ T·m and $I_2 = \int ds \int B_z ds' = 10^{-4}$ T·m^2 at a magnetic field of 0.1–0.3 T. The imperfection of the magnetic system produces excitations of electron trajectory of $x' \approx 0.05$ mrad and electron trajectory displacement of $x \approx 0.05$ mm at an electron energy of 0.7 GeV.

2. 2D SIMULATION OF THE FIRST INTEGRAL

The infra-red undulator magnetic field calculations were performed by 2D program POISSON [1] at the first stage, at the following stages by 3D RADIA code [2]. Two-dimensional code at a standard undulator geometry could not be used for simulation of the first integral. In 2D approach it always corresponds to zero. However, in reality the first integral of the dipole magnetic field is changed due to a leakage of a part of magnetic flux in the transverse direction. A two-dimensional modified model was created on the POISSON code base to estimate input in the first integral caused by mechanical accuracy at undulator construction. The section of the pole of the magnet was in the transverse direction (before medium of the pole) (Fig. 1), but hereinafter the undulator section is

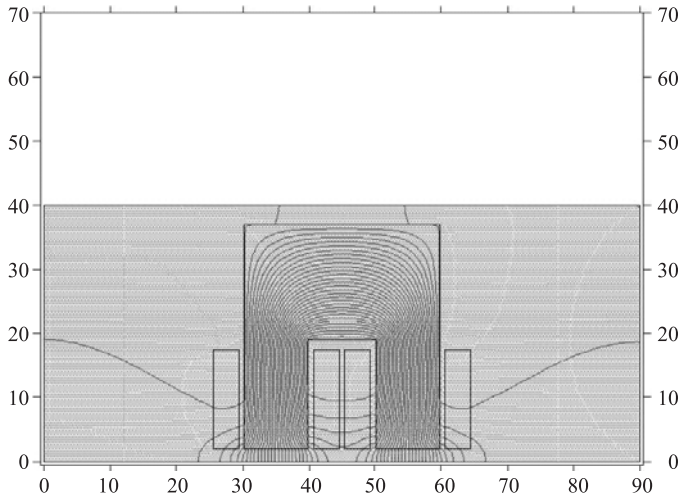

Fig. 1. 2D model of undulator (2D POISSON)

turned through 90° to the initial direction. The simulation of such two orthogonal undulator sections permits one to estimate an input of magnetic system errors on perturbation of the first and second integrals (see Table 1). At calculation of the magnetic field longitudinal integral, only a change of the flux corresponding to the transverse part of section was taken into account. The view of this model is given in Fig. 1.

3. 3D SIMULATIONS OF THE FIRST INTEGRAL

Calculations were performed of the influence for practically the whole spectrum of possible magnetic system errors by 3D code RADIA with different simulated number of undulator poles from 3 up 14 and with different degree of the symmetries. The 3-pole and 14-pole models are presented in Figs. 2 and 3. A magnetic field distribution along the undulator axis is presented in Figs. 4 and 5 at zero transverse coordinates $x = z = 0$.

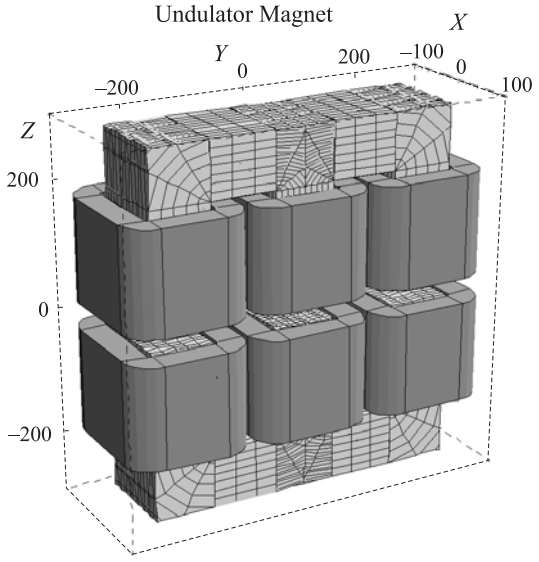

Fig. 2. RADIA model (3 poles)

Results of calculation are given in Table 1 for the different undulator magnetic system errors that influence on the first longitudinal integral of the dipole field. In the table we consider two types of errors related to mechanical accuracy at construction of different undualator elements. The first type of errors is connected with construction of undulator yoke. The input of yoke construction errors in value of the first integral is given in Table 1. The typical accuracy

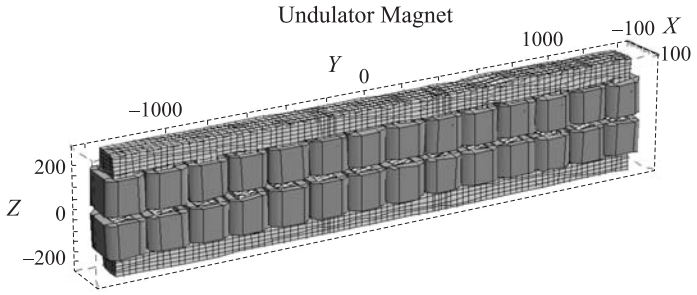

Fig. 3. RADIA model (14 poles)

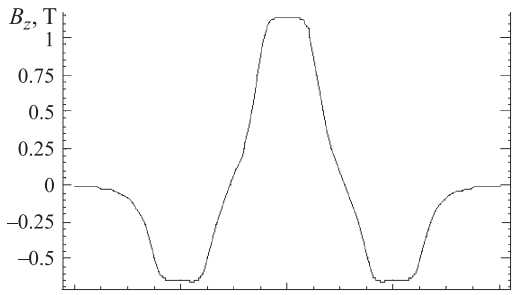

Fig. 4. The magnetic field distribution along the longitudinal axis (3 poles)

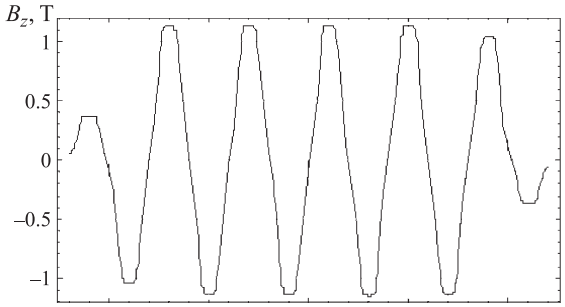

Fig. 5. The magnetic field distribution along the longitudinal axis (14 poles)

of mechanical construction for undulator yoke is less than 100 μm. The second type of errors is related to an accuracy at coil construction. The magnetic field in magnetic steel corresponds to 1.8–2.1 T at a dipole magnetic field of $B_z = 1.2$ T in the undulator gap. The magnetic steel in this case is oversaturated. A variation in the coil position or its size leads to a variation of the magnetic

Table 1. The input of undulator manufacturing errors in the first magnetic field integral

	POISSON $\Delta_{\rm int}$, G·cm $B_{\max} = 1.2$ T	RADIA 3 poles $\Delta_{\rm int}$, G·cm $B_{\max} = 1.2$ T	RADIA 5 poles $\Delta_{\rm int}$, G·cm $B_{\max} = 1.2$ T	RADIA 5 poles $\Delta_{\rm int}$, G·cm $B_{\max} = 0.1$ T
The poles gap increase (0.1 mm)	82	94	86	12
The transverse pole shift (0.1 mm)		14		
The transverse pole width decrease (0.1 mm)	30	36		
The longitudinal pole width decrease (0.1 mm)		50		
The pole turn in the horizontal plane (1.5 mrad)		~ 0		
The axial coil gap increase (1 mm)	364	262	342	12
The transverse coil size increase (1 mm)		42		
The longitudinal coil size increase (1 mm)		58		
The axial coil cross-section increase (1 mm)		58		
The transverse coil cross-section increase (1 mm)		8		
The transverse coil shift (1 mm)		36		
The coil turn in the horizontal plane (15 mrad)		2		

field distribution inside the undulator yoke and finally to a variation of dipole magnetic field in the undulator gap. This magnetic yoke induction of 1.8–2.1 T is rather specific case. The errors produced at coil construction usually do not give an input in the first and second integrals. To compensate excitation of the first and second integrals, the trim correction coils are used in each undulator pole. The typical value of dipole magnetic field without correction coils corre-

sponds to ±50 G. The current in correction coils provides the compensation of this magnetic field.

The axial coils offset excites stronger the first magnetic field integral. The models with different number of poles were used for determination of the possible model type influence on this kind of error simulation. The results are collected in Table 2. It follows from simulations that the range of integral change is 200–300 G·cm.

Table 2. The influence of vertical coil displacement (1 mm) on the field integral by the models with different number of poles

Field direction	Poles	6 poles Δ_{int}, G·cm	8 poles Δ_{int}, G·cm	10 poles Δ_{int}, G·cm	Average for all models, G·cm
↓	–P3			320	320
↑	–P2		321	320	320
↓	–P1	322	124	324	257
↑	P1	98	264	320	227
↓	P2		124	245	185
↑	P3			324	324

For simulation of the correction possibility of the given type of errors with the trim coil, the 10-pole model with random coil offset on the 6 central poles (maximum possible coil displacement is 1 mm) was used. The distribution of random undulator coil shift is presented in Fig. 6. The dipole magnetic field

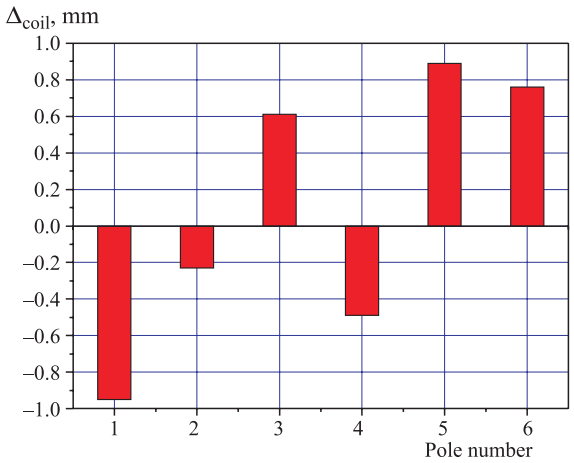

Fig. 6. Random offset distribution of the correction coils

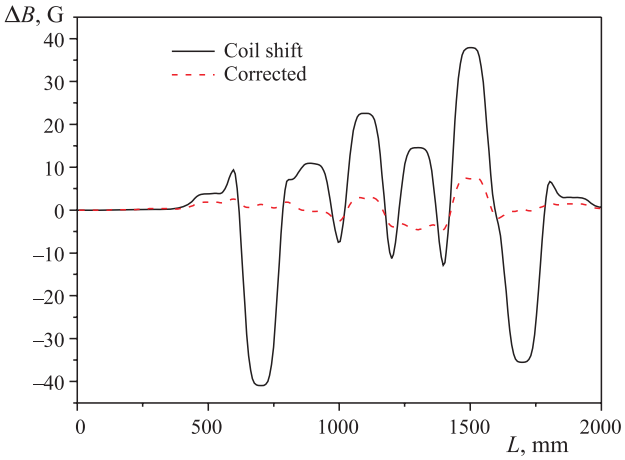

Fig. 7. Correction of the dipole field perturbation by trim coils

changes caused by undulator coil shift are given in Fig. 7 for two cases: without correction (solid line) and after correction (dotted line).

The application of correction coils permits one to reduce a few times the perturbed dipole magnetic field in the undulator gaps.

4. SIMULATIONS OF THE POLE SHAPE INFLUENCE

By 3D code the influence of the undulator pole shape on the magnetic field was studied. For getting the required value of the first field harmonic $B_1 = 1.2$ T the pole shape has to be chamfered. The direction and size of the chamfer has a deep influence on the value of third field harmonic. The view of the computer model for this kind of simulation is in Fig. 8. The results of simulation are summarized in Table 3 and in Figs. 9 and 10.

Table 3. Magnetic field parameters for different pole shapes

Pole shape	$B_{\max}$, T	B_1, T	B_3, T
Without chamfer	0.964	0.995	0.0455
Longitudinal chamfer (1/8 cm)	1.058	0.996	0.1447
Transverse chamfer (2/10 cm)	1.072	1.096	0.0584
Double transverse chamfer	1.172	1.179	0.0758

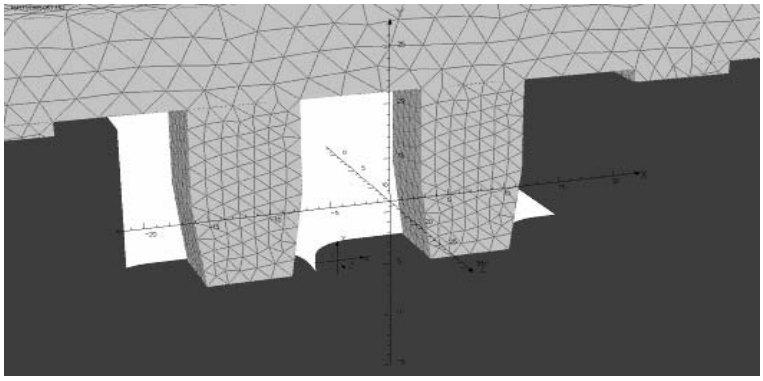

Fig. 8. 3D computer model for simulation of the pole shape effects

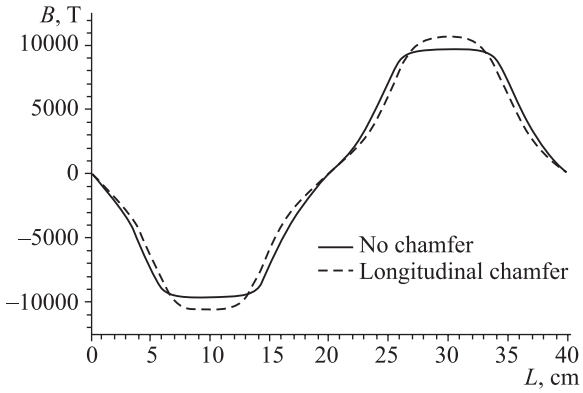

Fig. 9. Magnetic field for the pole without chamfer and with longitudinal one

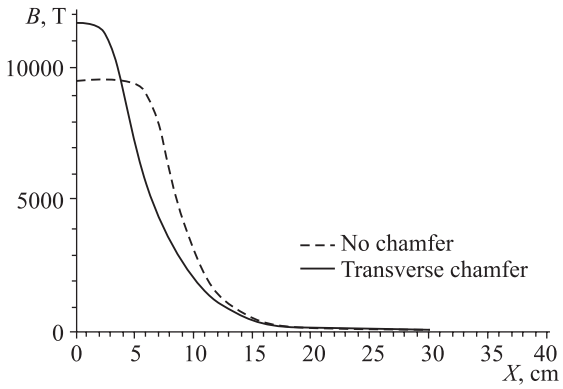

Fig. 10. Magnetic field for the transverse pole chamfer

CONCLUSIONS

- On the basis of the simulation results it is possible to recommend an accuracy for the ferromagnetic undulator elements of ~ 0.1 mm, for coils ~ 1 mm.
- For initial correction of dipole magnetic field disturbance it is appreciable to use a small moving of the coils and this possibility has to be reserved in the undulator design.
- The preferable pole chamfering is in the transverse direction.

REFERENCES

1. *Billen I. H., Young L. M.* POISSON SUPERFISH Documentation, LA-UR-96-1834. Los-Alamos, 1996.
2. *Chavanne J., Chubar O., Elleaume P.* RADIA, a 3D Magnetostatic Computer Code, IMMW-12, ESRF, Grenoble, France, 2001.

Received on October 28, 2005.

Редактор *Е. И. Кравченко*

Подписано в печать 20.01.2006.
Формат 60 × 90/16. Бумага офсетная. Печать офсетная.
Усл. печ. л. 0,69. Уч.-изд. л. 0,99. Тираж 270 экз. Заказ № 55192.

Издательский отдел Объединенного института ядерных исследований
141980, г. Дубна, Московская обл., ул. Жолио-Кюри, 6.
E-mail: publish@pds.jinr.ru
www.jinr.ru/publish/